# Quantum Necking in Stressed Nanowires

J. Bürki,[1] Raymond E. Goldstein,[1,2] and C. A. Stafford[1]
[1] *Department of Physics and* [2] *Program in Applied Mathematics, University of Arizona, Tucson, AZ 85721*
(Dated: September 30, 2002)

When a macroscopic metallic wire is subject to tensile stress, it necks down smoothly as it elongates. Here we show that for nanowires with radii comparable to the Fermi wavelength $\lambda_F$, this process is remarkably different. Using a new semiclassical energy functional to include electron-shell effects, we formulate a PDE for the shape evolution of a nanowire using concepts from fluid dynamics. Extensional and compressional stress lead to unusual shape dynamics, characterized by interacting kinks connecting locally stable radii, and hysteresis, the latter in accord with recent experiments on gold nanowires.

PACS numbers: 47.20.Dr, 61.46.+w, 68.35.Ja, 68.66.La

Recently, it has become possible to image metal nanowires with subatomic resolution, and record their structural evolution in real time, using transmission-electron microscopy [1, 2, 3, 4, 5], thus opening the door to the study of a new class of nonlinear dynamical phenomena at the nanoscale. Heretofore, most of the information about the structure and dynamics of nanowires has been obtained indirectly, from measurements of transport and/or cohesive properties [6, 7, 8, 9, 10]. Molecular dynamics simulations [11, 12, 13, 14] have also provided important insight into the atomic structure and dynamics of nanowires, but cannot explain the observed stability [1, 3, 5] of long, cylindrical nanowires, which would be unstable classically under surface tension [15].

The free-electron approach to nanowires [16, 17, 18, 19], on the other hand, has proven successful in explaining the quantum suppression of the Rayleigh instability [18]. Here we extend this approach by developing a structural dynamics for a free-electron nanowire, based on the assumption that surface diffusion is the dominant process. This dynamics, of interest on its own as a new class of non-linear dynamics, includes quantum-size effects explicitly and allows the study of a broad range of dynamical effects in metallic nanowires (see Fig. 1(b-d)): Approach to equilibrium of a point contact, roughening of an unstable nanowire [19], and evolution of a wire under elongation/compression. In particular, the latter can be compared to early experiments on gold point contacts [6, 7], showing perfect correlation between force and conductance with steep conductance steps, and a hysteresis between elongation and compression.

More specifically, our model of a nanowire consists of free electrons confined to an axially-symmetric wire by a hard-wall potential [16]. The shape of the wire is described by its radius $R(z,t)$ in an interval $[0,L]$, the $z$-axis being chosen parallel to the wire. Periodic boundary conditions are used to extend $R(z)$, although contacts such as those depicted in Fig. 1 (b) and (d) are to be seen as connected to semi-infinite, cylindrical leads [21]. The restriction to axially-symmetric wires is motivated physically by the fact that classically, Jahn-Teller-type deformations of a wire are energetically less favorable than axially-symmetric deformation [15].

In order to find the equilibrium shape of a nanowire, one needs to minimize its energy as a functional of $R(z)$. In the spirit of the Born-Oppenheimer approximation, the total energy of the nanowire is taken to be the electronic energy. Since we are dealing with an open system of electrons, the grand-canonical potential is used, and can be separated into Weyl and mesoscopic contributions [17, 22]. Dropping the volume contribution, which is assumed to be constant, we find that the energy functional

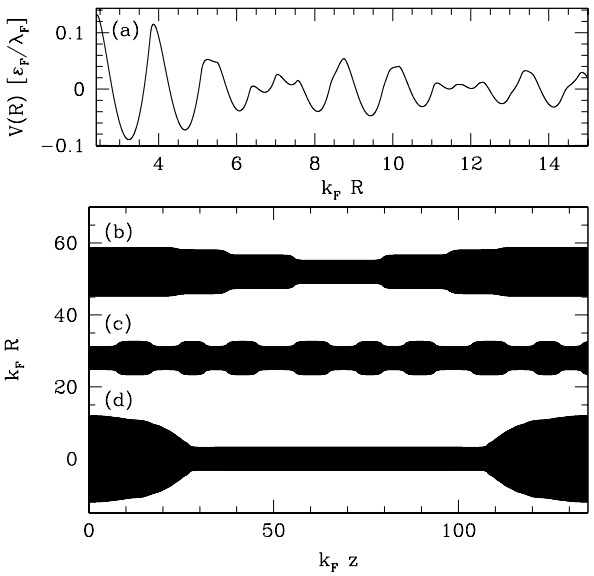


FIG. 1: (a) Electron-shell potential $V(T,R)$ as a function of radius for a temperature $T = 2 \cdot 10^{-3} T_F$. Here $\varepsilon_F$ is the Fermi energy, $T_F = \varepsilon_F / k_B$ and $k_F = 2\pi/\lambda_F$. (b)-(d) Various equilibrium shapes [20] of a nanowire: (b) Shape obtained starting from a double-cone geometry; (c) Roughening of an unstable cylinder with starting radius $k_F R = 4$; (d) Shape obtained dynamically through elongation of a constriction.

may be written

$$\Omega\big[T,R(z)\big] = \sigma(T)\mathcal{S}\big[R(z)\big] + \int_0^L V\big(T,R(z)\big)\mathrm{d}z, \quad (1)$$

where $\sigma(T)$ is the surface tension [23], $\mathcal{S}$ is the surface area of the wire, and $V$ is a mesoscopic electron-shell potential. Higher-order terms [17, 22] proportional to the mean curvature, etc., are neglected. $V$ can be expressed in terms of a Gutzwiller-type trace formula as

$$V(T,R) = \frac{2\varepsilon_F}{\pi} \sum_{\substack{w\geqslant 1 \\ v\geqslant 2w}} a_{vw}(T)\frac{f_{vw}\cos\theta_{vw}}{v^2 L_{vw}}, \quad (2)$$

where the sum includes all classical periodic orbits $(v,w)$ in a disk billiard [22], characterized by their number of vertices $v$ and winding number $w$, $L_{vw} = 2vR\sin(\pi w/v)$ is the length of orbit $(v,w)$, and $\theta_{vw} = k_F L_{vw} - 3v\pi/2$. The factor $f_{vw} = 1+\theta(v-2w)$ accounts for the invariance under time-reversal symmetry of some orbits, and $a_{vw}(T) = \tau_{vw}/\sinh\tau_{vw}$ ($\tau_{vw} = \pi k_F L_{vw} T/2T_F$) is a temperature-dependent damping factor. $V(R)$, shown in Fig. 1(a), has deep minima that favor some magic radii [9]. A similar trace formula was previously derived [18] for small axially-symmetric perturbations of a cylinder using semiclassical perturbation theory [22, 24, 25]. Here we point out that semiclassical perturbation theory remains valid for large deformations, as long as new classes of non-planar orbits can be neglected (adiabatic approximation). Eqs. (1) and (2) define an energy functional which is both general enough and simple enough to solve for nontrivial nanowire geometries.

Rather than directly minimizing the energy functional (1), we derive an equation describing the surface dynamics of the nanowire, which will yield not only the equilibrium shapes, but also the approach to equilibrium and the onset of instability. Our model contains two main assumptions. First, the majority of atoms are at the surface in the thin wires under consideration, so we focus on surface self-diffusion as the origin of ionic motion. Second, under the Born-Oppenheimer approximation, the electronic energy (1) acts as a potential for the ions, and we derive the dynamics from ionic mass conservation:

$$\frac{\partial R(z,t)}{\partial t} = -\frac{v_a}{R(z,t)}\frac{\partial}{\partial z}\big[R(z,t)J_z(z,t)\big], \quad (3)$$

where $v_a = 3\pi^2/k_F^3$ is the volume of an atom, and the $z$-component of the surface current is given by Fick's law:

$$J_z = -\frac{\rho_S D_S}{k_B T}\big[1+(R')^2\big]^{-1}\frac{\partial\mu}{\partial z}, \quad (4)$$

where $R' = \partial R/\partial z$, and $\rho_S$ and $D_S$ represent the surface density of ions and the surface self-diffusion coefficient, respectively. It appears that the precise value of $D_S$ for alkali metals is not known, but we can remove it explicitly from the evolution equation by a suitable rescaling of time. Accordingly, all times in this paper will be given as a dimensionless variable $\tau = \rho_S D_S T_F t/T$. The chemical potential $\mu(z_0)$ is obtained by calculating the change in the energy (1) with the addition of an atom at point $z_0$, $\mu(z_0) \equiv \Omega\big[T,R(z)+A\delta(z-z_0)\big] - \Omega\big[T,R(z)\big]$, where $A = v_a/2\pi R$ is chosen so that the volume of an atom is added:

$$\mu(z) = -\frac{2\varepsilon_F}{5} + \frac{3\pi\sigma}{k_F^3 R(z)\sqrt{1+R'^2}}\Big(1-\frac{RR''}{1+R'^2}\Big) - \frac{3\varepsilon_F}{k_F^2 R^2}\sum_{\substack{w\geqslant 1 \\ v\geqslant 2w}} \frac{a_{vw}f_{vw}}{v^2}\left[\sin\theta_{vw} + b_{vw}\frac{\cos\theta_{vw}}{k_F L_{vw}}\right], \quad (5)$$

where $b_{vw}(T) = a_{vw}\cosh\tau_{vw}$. Eq. (3) is then solved numerically using a linearized implicit scheme.

Let us first explore the equilibrium shape of a nanowire: Some insight can be obtained by expanding the energy functional (1) in the perturbation $\phi(z) = R(z) - R_0$ about a cylinder of radius $R_0$. The surface term in Eq. (1) contributes a term $\propto(\partial\phi/\partial z)^2$, while the electron-shell potential $V(T,\phi)$ may be approximated locally by a cosine, leading to a sine-Gordon energy [26]. This suggests solutions where $R(z)$ is piece-wise constant, with segments of different radius connected by kinks. This is confirmed by solving Eq. (3) numerically: Starting from a double-cone shape, one finds [Fig. 1(b)] a local minimum of the energy consisting of a series of cylindrical sections separated by steps whose length is proportional to $R_0$. The distance between the steps depends on the initial conditions, but the general features of the solution are robust.

Another case of interest is the roughening of an unstable nanowire [19], or the propagation of an instability [27]: Starting with a cylinder with an unstable radius, corresponding to a maximum in $V(R)$ [Fig. 1(a)], and adding a localized (gaussian in shape) deformation of small amplitude (0.1% of the wire radius), we find that,

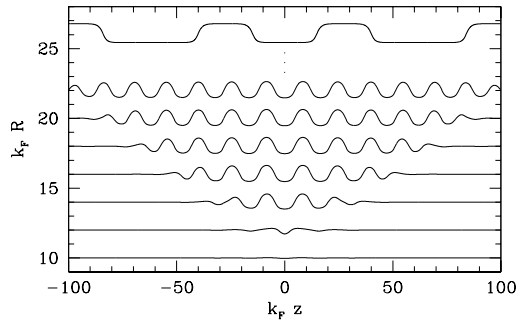


FIG. 2: Propagation of an instability for a wire of initial radius $k_F R = 10$, time progressing from bottom to top, with curves shifted for clarity. The top curve corresponds to a much later stage in the time evolution.

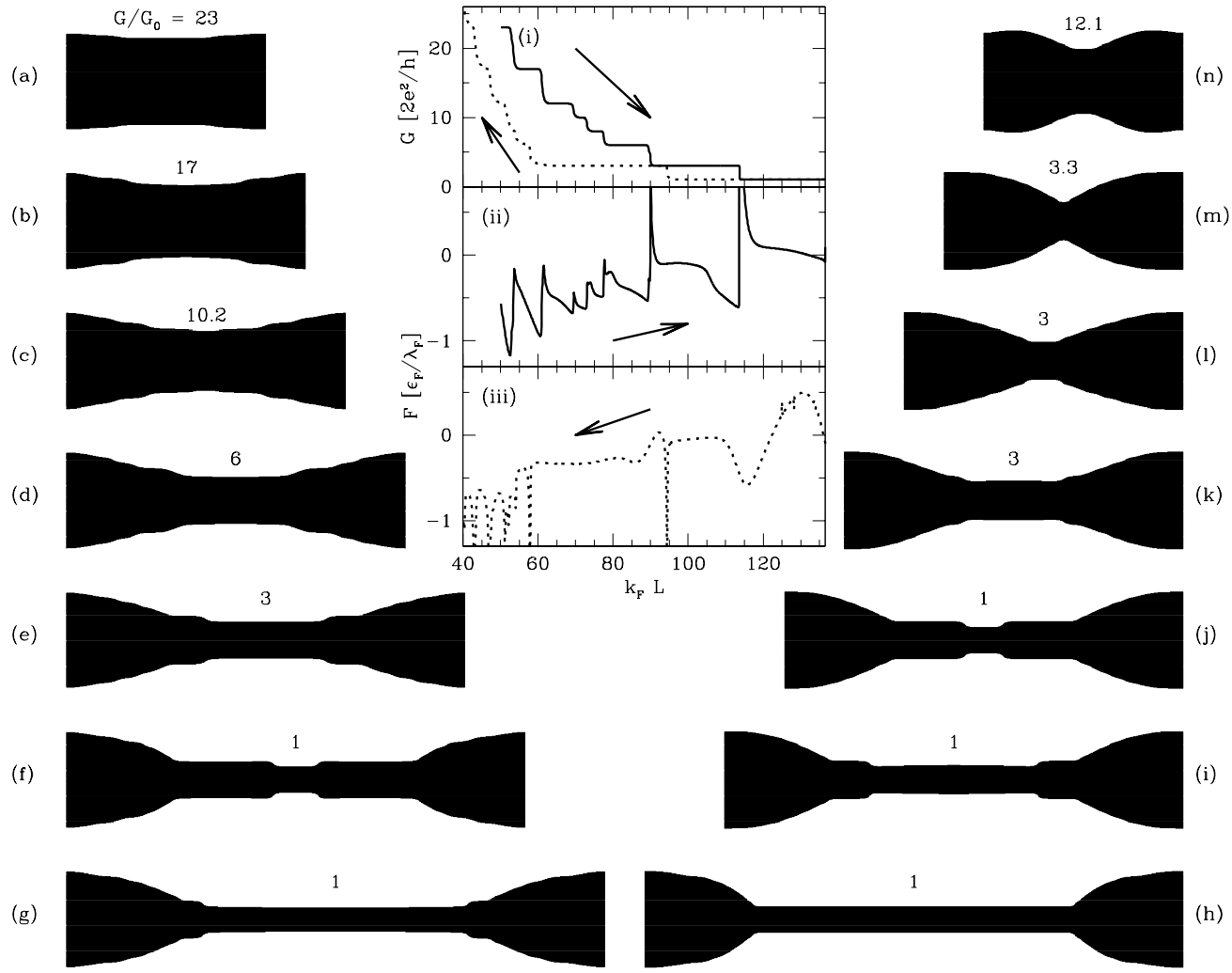


FIG. 3: Shape of a nanowire at various stages [20] of elongation (left column, a-g) and subsequent compression (right column, h-n). Adjacent wires have the same length, from top to bottom: $k_F L = 50, 60, 70, 85, 100, 115, 135$. Above each wire is its conductance in units of $G_0 = 2e^2/h$. Central Inset: Conductance and force as a function of the length of the wire: (i) Conductance during elongation (solid line) and compression (dotted line); (ii) force during elongation; (iii) force during compression.

after an incubation period during which the perturbation decreases, the instability sets in with essentially a single Fourier component, corresponding to the maximally unstable mode [19], saturates at a finite amplitude, and propagates with a constant velocity (see Fig. 2). This is exactly how classical analogs of this instability can behave, such as the pearling instability of membranes [28, 29]. The classical Rayleigh instability itself [27] propagates in a similar way, but does not saturate, instead leading to breakup of the cylinder. Both the front velocity and wavelength of the instability are strongly dependent on the initial radius [19]. Once the instability is fully developed, kink-antikink pairs start annihilating, eventually leading to a shape consisting of a series of cylinders of different radii [corresponding to neighboring minima in $V(R)$, Fig. 1(a)], connected by kinks. Starting from a more realistic initial condition with random perturbations, the instability occurs at several places more or less simultaneously, but the amplitude still saturates, dominated by a single Fourier component.

The dynamical model also allows for the study of the evolution of a nanowire under stress. Stress is simulated by changing the length $L$ of the wire at a constant rate $u = dL/dt$, while rescaling the radius $R(z)$ in order to keep the volume constant. We start with a double-cone constriction of length $k_F L = 50$, which we let equilibrate according to Eq. (3) [see Fig. 3(a)]. We then stress the wire by elongating it at a constant speed $k_F dL/d\tau = 0.1$ until it is close to breaking [Fig. 3(b-g)], at which point we let it equilibrate again [Fig. 3(h)]. Subsequently, we compress the wire at the same rate until returning approximately to a cylindrical wire [Fig. 3(i-n)]. During

elongation, the necking of the wire occurs by nucleation of kink-antikink pairs at the center of the wire [30], with subsequent motion of these kinks toward the leads, leaving a long, cylindrical wire in the middle. During compression, the reverse process occurs so long as the central, cylindrical section is long enough: Kinks move out of the leads toward the center, where they annihilate. Once the cylindrical part gets too short, kinks are just pushed by the leads and can not be distinguished from them.

These different processes lead to a substantial hysteresis between elongation and compression, as can be seen by computing the electrical conductance of the contact and the force applied to it. The force is obtained from the change in the energy (1) with elongation, $F = -\partial\Omega/\partial L$. The conductance is computed from the Landauer formula [31], using the adiabatic and WKB approximations [16] to compute the transmission probabilities. Both quantities are shown in the central inset of Fig. 3. Compared to our previous results obtained without optimization of the shape [16], the conductance steps and relaxations of the force are much steeper, in better agreement with experiments [6], and a substantial hysteresis is observed in the conductance. It has been argued [6, 8] that the abruptness of the conductance steps, and their perfect correlation with the jumps in the force, rule out an electronic mechanism. However, we have shown that this behavior arises naturally in a model which takes proper account of electronic quantum-size effects on the structure, even when atomistic effects are neglected.

A final interesting feature is the spikes in the force that occur at the opening and closing of a channel, corresponding to the rapid energy relaxation during the creation or annihilation of a kink/antikink pair. These spikes are suppressed, and the hysteresis decreases, when the speed of deformation is increased, suggesting that the spikes might be observable experimentally by decreasing the elongation rate. A failure of this model is the force during compression: contrary to experiment [6, 8], the force is attractive, suggesting that a resistance to compression due to the ions needs to be added to the free-electron model. Indeed, an interesting question raised by this work is how discrete positive ions would arrange themselves to accomodate the predicted shapes favored by the conduction electrons.

This research was supported in part by NSF grant DMR0072703 and by an award from Research Corporation (CAS), and by NSF grant DMR9812526 (REG). JB acknowledges support from the Swiss National Science Foundation.

[1] Y. Kondo and K. Takayanagi, Phys. Rev. Lett. **79**, 3455 (1997).
[2] T. Kizuka, Phys. Rev. Lett. **81**, 4448 (1998).
[3] Y. Kondo and K. Takayanagi, Science **289**, 606 (2000).
[4] V. Rodrigues and D. Ugarte, Phys. Rev. B **63**, 073405 (2001).
[5] V. Rodrigues and D. Ugarte, Phys. Stat. Sol. (b) **230**, 475 (2002).
[6] G. Rubio, N. Agraït, and S. Vieira, Phys. Rev. Lett. **76**, 2302 (1996).
[7] A. Stalder and U. Dürig, Appl. Phys. Lett. **68**, 637 (1996).
[8] C. Untiedt, G. Rubio, S. Vieira, and N. Agraït, Phys. Rev. B **56**, 2154 (1997).
[9] A. I. Yanson, I. K. Yanson, and J. M. van Ruitenbeek, Nature **400**, 144 (1999).
[10] A. I. Yanson, I. K. Yanson, and J. M. van Ruitenbeek, Phys. Rev. Lett. **84**, 5832 (2000).
[11] U. Landman, W. D. Luedtke, N. A. Burnham, and R. J. Colton, Science **248**, 454 (1990).
[12] T. N. Todorov and A. P. Sutton, Phys. Rev. B **54**, R14234 (1996).
[13] M. R. Sørensen, M. Brandbyge, and K. W. Jacobsen, Phys. Rev. B **57**, 3283 (1998).
[14] O. Gülseren, F. Ecrolessi, and E. Tosatti, Phys. Rev. Lett. **80**, 3775 (1998).
[15] S. Chandrasekhar, *Hydrodynamic and Hydromagnetic Stability* (Dover, New York, 1981), pp. 515–74.
[16] C. A. Stafford, D. Baeriswyl, and J. Bürki, Phys. Rev. Lett. **79**, 2863 (1997).
[17] C. A. Stafford, F. Kassubek, J. Bürki, and H. Grabert, Phys. Rev. Lett. **83**, 4836 (1999).
[18] F. Kassubek, C. A. Stafford, H. Grabert, and R. E. Goldstein, Nonlinearity **14**, 167 (2001).
[19] C. H. Zhang, F. Kassubek, and C. A. Stafford, cond-mat/0209601.
[20] The complete simulations can be viewed at, URL `http://www.physics.arizona.edu/~stafford/necking.html`.
[21] The locality of the semi-classical energy functional, Eq. (1), suppresses the dependence on boundary conditions of the electron gas.
[22] M. Brack and R. K. Bhaduri, *Semiclassical Physics* (Addison-Wesley, Reading, MA, 1997).
[23] In the simulations, the value $\sigma = \varepsilon_F k_F^2/80\pi$ was used [17], which is a good approximation for alkali metals. For noble metals, $\sigma$ is roughly twice as large.
[24] D. Ullmo, M. Grinberg, and S. Tomsovic, Phys. Rev. E **54**, 136 (1996).
[25] S. C. Creagh, Ann. Phys. **248**, 60 (1996).
[26] P. M. Chaikin and T. C. Lubensky, *Principles of condensed matter physics* (Cambridge University Press, 1995), p. 599.
[27] D. Zhang, T. Powers, R. Goldstein, and H. Stone, Phys. Fluids **10**, 1052 (1998).
[28] R. Bar-Ziv and E. Moses, Phys. Rev. Lett. **73**, 1392 (1994).
[29] R. Goldstein, P. Nelson, T. Powers, and U. Seifert, J. Phys. II (France) **6**, 767 (1996).
[30] The mirror-symmetry of the wire about its thinnest point follows from the ansatz for elastic rescaling under stress that we employ, and the symmetrical initial shape.
[31] S. Datta, *Electronic Transport in Mesoscopic Systems* (Cambridge University Press, 1995), pp. 48–170.